Journal of Biomedical Optics

BiomedicalOptics.SPIEDigitalLibrary.org

Ion-imprinted nanoparticles for the concurrent estimation of Pb(II) and Cu(II) ions over a two channel surface plasmon resonance-based fiber optic platform

Anand Mohan Shrivastav
Banshi D. Gupta

SPIE.

Anand Mohan Shrivastav, Banshi D. Gupta, "Ion-imprinted nanoparticles for the concurrent estimation of Pb (II) and Cu(II) ions over a two channel surface plasmon resonance-based fiber optic platform," *J. Biomed. Opt.* **23**(1), 017001 (2018), doi: 10.1117/1.JBO.23.1.017001.

Ion-imprinted nanoparticles for the concurrent estimation of Pb(II) and Cu(II) ions over a two channel surface plasmon resonance-based fiber optic platform

Anand Mohan Shrivastav and Banshi D. Gupta*
Indian Institute of Technology Delhi, Department of Physics, New Delhi, India

Abstract. We report the design, fabrication, and characterization of an optical fiber sensor based on the surface plasmon resonance (SPR) technique for the simultaneous determination of lead (Pb) and copper (Cu) metal ions in aqueous samples. Two cascade channels over a single optical fiber are fabricated by removing cladding from two well-separated regions of the fiber. SPR working as a transducing mechanism for the sensor is realized by coating thin films of copper and silver over unclad cores of channel I and channel II, respectively. Ion-imprinted nanoparticles for both ions are separately synthesized and coated over the metal-coated unclad cores of the fiber as the recognition layers for sensor fabrication. A first channel having layer of Pb(II) ion-imprinted nanoparticles detects Pb(II) ions and a second channel having layer of Cu(II) ion-imprinted nanoparticles are used for the detection of Cu(II) ions. Both channels are characterized using the wavelength interrogation method. The sensor operates in the range between 0 to 1000 μg/L and 0 to 1000 mg/L for Pb(II) and Cu(II) ions, respectively. These ranges cover water resources and the human body for these ions. The sensitivities of channel I and channel II are found to be 8.19×10^4 nm/(μg/L) and 4.07×10^5 nm/(mg/L) near the lowest concentration of Pb(II) and Cu(II) ions, respectively. The sensor can detect concentrations of Pb(II) and Cu(II) ions as low as 4.06×10^{-12} g/L and 8.18×10^{-10} g/L, respectively, which are the least among the reported values in the literature. Further, the probe is simple, cost effective, highly selective, and applicable for online monitoring and remote sensing. [DOI: 10.1117/1.JBO.23.1.017001]

Keywords: optical fiber sensor; surface plasmon resonance; ion-imprinted nanoparticles; multichannel sensing; lead ions; copper ions.

Paper 170592R received Sep. 15, 2017; accepted for publication Dec. 13, 2017; published online Jan. 8, 2018.

1 Introduction

The presence of heavy metal ions in the atmosphere and foodstuffs is a serious topic of concern due to the safety of human health because these are highly toxic or poisonous chemical components having a low density.[1] The metals with atomic weights in the range from 63 to 200 g/mol are usually called heavy metals and a few of these are lead, copper, cadmium, zinc, and manganese.[2] These metals are biodegradable and universally distributed in the atmosphere. Their ions enter living species through alimentary chains and affect human health due to their toxic nature. In the human body, these ions interact with the thiol group of proteins and affect their life cycles, even at very low concentrations.[3,4] Among the heavy metal ions, lead [Pb(II)] ion is a well-known neurotoxin, and its higher concentration may cause various diseases such as hypertension, neurological damage, cognitive dysfunction, and neurobehavioral disorders.[5] Further, copper [Cu(II)] ion is an essential nutrient for the human body and plays a significant role in the various enzymatic processes. Its deficiency and excess in the human body are also very harmful.[6] Due to these reasons, the accurate determination of their concentrations is an important topic of research. A number of detection schemes have been reported in the literature for the detection of lead and copper ions. These methods include IR spectroscopy, colorimetry, reverse transcription polymerase chain reaction (RT-PCR) technology, UV–vis spectroscopy, and electrochemical analysis.[7–15] Although these methods are sensitive and stable, they suffer from being complex, high cost, laborious and time consuming, tedious, and incapable of simultaneous detection of different metal ions. Therefore, the development of a simple, low cost, highly sensitive, and selective sensor that can detect both ions (lead and copper) simultaneously is the requirement at the present time.

In recent years, molecularly imprinted nanoparticles in collaboration with the surface plasmon resonance (SPR) technique have shown potential application in the detection of various molecules. Molecularly imprinted nanoparticles are the polymeric nanoparticles possessing vacant binding sites of reciprocal shape and size of the template molecule to be detected.[16] These binding sites act as the recognition memory encampments for the template molecule due to complementary shape and size. The advantages are high selectivity, easy synthesis process, high stability, and physical robustness.[17] Further, the nanosized particles provide better accessibility of the template toward molecular recognition due to the increased aspect ratio. When the template molecule comes near the vicinity of these binding

*Address all correspondence to: Banshi D. Gupta, E-mail: bdgupta@physics.iitd.ac.in

1083-3668/2018/$25.00 © 2018 SPIE

sites of the molecularly imprinted nanoparticles, they interact with the sites through covalent or noncovalent interaction, changing the optical properties of polymeric nanoparticles.[16,18] The change in the optical properties due to the change in the concentration of the template molecule around the polymeric nanoparticles is determined using the SPR phenomenon.[19] In the case of imprinting of ions, the technique is referred to as ion imprinting and the corresponding nanoparticle is called ion-imprinted nanoparticle.

The SPR technique has been widely used for sensing applications in the last three decades because of high sensitivity, simple design, low cost, label-free sensing, etc.[20–23] Surface plasmons are the quanta of in-phase oscillating free electrons at the metal–dielectric interface. These oscillations are longitudinal in nature and can be excited by *p*-polarized light. In the fiber optic configuration, these oscillations, produced at the interface of metal-coated core and dielectric medium, are excited by the exponentially decaying evanescent field produced at the core–metal interface due to the total internal reflection of the light guided through the fiber core. The matching of the propagation vectors of evanescent wave (at the core–metal interface) and the surface plasmon wave (at the metal–dielectric interface) results in the SPR. At resonance, surface palsmons get excited and some part of the light guided through the core of the fiber is transferred to the metallic medium, which causes a sharp attenuation dip at a specific wavelength in the transmitted spectrum of the light. The wavelength corresponding to the dip, termed the resonance wavelength, depends on the optical properties (dielectric constant) of the dielectric medium around the metallic film. The resonance wavelength changes according to the variation in the dielectric constant of this medium. Thus, by observing the change in the resonance wavelength, the change in the dielectric constant or refractive index of the medium around the metal layer can be determined. The SPR-based fiber optic sensors are advantageous due to their application in simultaneous detection of two analytes by fabricating the two sensing channels over a single optical fiber platform. Our group has earlier reported the simultaneous detection of two analytes using SPR-based optical fiber configuration.[24,25] Two channels have coatings of two different metals so that two distinct SPR dips in the transmitted spectrum can be obtained. To sense the analytes, the metal layers are further coated with analyte-sensitive dielectric layers. A change in the concentration of one of the two analytes changes the resonance wavelength of one dip, whereas the change in the concentrations of both analytes changes the resonance wavelengths of both dips. By knowing the shifts in resonance wavelengths of both dips, the concentrations of both analytes can be determined. The fiber optic platform is beneficial due to the various other factors such as low cost, light weight, electromagnetic interference immunity, applicability of the probe for *in vivo* and *in vitro* applications, and the possibility of online monitoring and remote sensing.

In the present work, design, fabrication, and characterization of an SPR-based fiber optic multichannel sensor for the simultaneous detection of Pb(II) and Cu(II) ions using ion-imprinted nanoparticles are reported. The sensor probe contains two cascade channels for the detection of Pb(II) and Cu(II) ions. The channels are fabricated over a single fiber by removing cladding from the two well-separated regions of the fiber and coating them with two different metals. The first unclad region is coated with copper film, while the second one with silver film. To fabricate sensing layers, the copper and silver layers are coated with the layer of Pb(II) ion- and Cu(II) ion-imprinted nanoparticles, respectively. Thus, the first channel senses Pb(II) ions, while the second channel is for Cu(II) ions. The characterization of the probe is carried out using the wavelength interrogation method, while the concentration range of Pb(II) and Cu(II) ions is kept as 0 to 1000 μg/L and 0 to 1000 mg/L, respectively.

2 Materials and Methods

2.1 *Reagents*

Highly multimode plastic clad silica (PCS) fiber was procured from Fiberguide Industries. The core diameter and numerical aperture of the optical fiber were 600 μm and 0.37, respectively. Epichlorohydrin, branched polyethyleneimine (PEI) (average molecular weight = 25 kDa), aqueous ammonia (NH_4OH), and ethylene diamine tetra-acetic acid (EDTA) were purchased from Sigma Aldrich. Hydrochloric acid, sodium hydroxide (NaOH), copper nitrate trihydrate [$Cu(NO_3)_2.3H_2O$], lead nitrate [$Pb(NO_3)_2$], copper powder (99% pure), and other metal salts were obtained from Fisher Scientific. 99.99% pure Silver (Ag) wire was procured from Sigma Aldrich Chemicals. No further purification of the above chemicals was performed before the experiments.

2.2 *Synthesis of Nonimprinted Nanoparticles*

Synthesis of Cu(II) ion-imprinted nanoparticles was performed using little modification in the procedure reported in the literature.[26,27] Initially, oligomer of epichlorohydrin amine (ECHA) was prepared by dropwise mixing of 1 mol of aqueous ammonia solution in 2 mol of epichlorohydrin at 60°C under rigorous stirring for 4 h. Further, 3.025 g of $Cu(NO_3)_2.3H_2O$ was dissolved in 30 ml of deionized water and 5 g of PEI was added to the solution. This solution was then kept for ultrasonication for 30 min. The earlier prepared ECHA oligomer was then added at 80°C with constant stirring for 4 h. This step completed the preparation of nonimprinted (NIP) nanoparticles having Cu(II) ions freeze within its vicinity. For seeking the size distribution of polymeric nanoparticles, the transmission electron microscope (TEM) analysis of synthesized nanoparticles

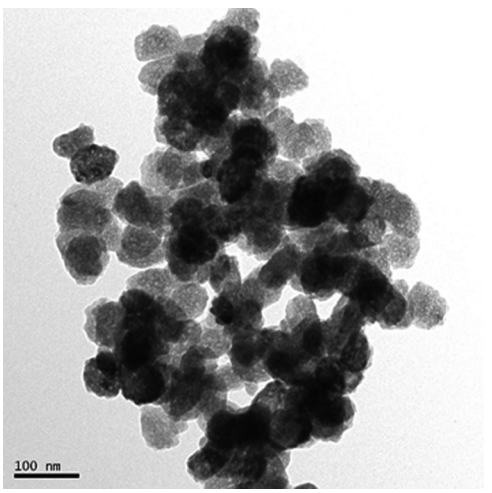

Fig. 1 TEM micrograph of polymeric nonimprinted nanoparticles with Cu(II) ions within its vicinity.

was performed. Figure 1 shows the TEM micrograph of the nanoparticles and from the micrograph, the sizes of the nanoparticles were found to be in the range from 50 to 70 nm.

NIP nanoparticles with Pb(II) ions were also prepared in a similar manner using $Pb(NO_3)_2$ as the template. To create the imprinted sites of metal ions in these nanoparticles, the removal of these ions was performed in the further steps of the probe fabrication process.

2.3 *Fabrication of Fiber Optic Probe*

For fabrication of the probe, PCS fiber with around 20-cm length was used and two separated regions of that fiber were uncladed using a sharp stainless-steel blade. The length of each unclad portion was ~1 cm. The first unclad portion was termed channel I, while the other unclad portion was named channel II. Both channels were cleaned by repeated washing with acetone and methanol for the removal of any external contamination. The coatings of 40-nm-thick copper film over channel I and 40-nm-thick silver film over channel II were performed. The coatings were performed by the thermal evaporation process, and during deposition the chamber pressure was maintained at 5×10^{-6} mbar. The coating unit contains a digital thickness monitor setup with quartz crystal microbalance, which was used to monitor the deposition rate and thickness of the films coated. The deposition rate for the coating of both films was kept around 0.04 nm/s to ensure the uniformity of the films. Further, the coating of NIP nanoparticles over the metal films was performed using the dip coating method. NIP nanoparticles having Pb(II) ions were coated over channel I, while Cu(II) NIP nanoparticles were coated over channel II. The dip coating was performed by vertically dipping the metal layer coated channel in the corresponding NIP nanoparticle solution for 30 min. The NIP nanoparticles-coated probe was left overnight for drying. The imprinting of Pb(II) and Cu(II) ions was performed by repeatedly washing the probe with 0.1-M hydrochloric acid and EDTA. After washing, the probe was left for 12 h to dry. This completed the probe fabrication process. A schematic of the fabricated probe is shown in Fig. 2(a).

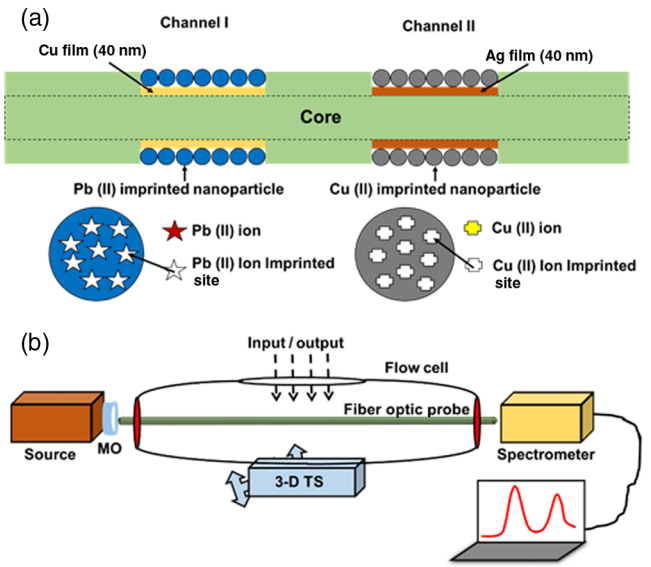

Fig. 2 Schematic of (a) fabricated sensing probe and (b) experimental setup for the probe characterization.

2.4 *Experimental Instrumentation*

The characterization of the fabricated probe using the method mentioned in the above section was performed using the experimental setup shown in Fig. 2(b). Before performing the experiments, both ends of the fiber optic probe were cleaved for maximum guidance of the light through the fiber. This was done by a sharp tungsten cutter. Now, the sensor probe was fixed with a flow cell, which had facilities of the inlet and outlet of the aqueous samples. Thus, the samples easily interacted with the sensing region of the fiber optic probe. The flow cell was mounted over a three-dimensional translational stage (3D-TS) so that maximum light could be coupled through the fiber.

Light from a polychromatic source (tungsten halogen lamp) was launched through the one end of the fiber and the output spectrum was recorded using a spectrometer (Avaspec-3648), which was interfaced with a laptop. Aqueous samples of Pb (II) and Cu(II) with a concentration range of 0 to 1000 μg/L and 0 to 1000 mg/L, respectively, were prepared for the characterization of the probe.

3 Results and Discussion

3.1 *Fundamental of Sensing*

The sensing of Pb(II) and Cu(II) ions is based on the interaction of ions with corresponding ion-imprinted nanoparticles. When the solution of the metal ions comes near the ion-imprinted nanoparticle layer, metal ions bind noncovalently with corresponding complementary binding sites and cause the change in effective refractive index of the sensing layer (ion-imprinted nanoparticle layer). The change in effective refractive index causes the shift in peak absorbance wavelength of the spectrum recorded. In the present probe, two cascade channels have been fabricated over a single fiber named channel I and channel II. Channel I has the configuration of core/Cu/Pb(II) ions-imprinted nanoparticles, while channel II consists of the layers of Ag/Cu(II) ions-imprinted nanoparticles over an unclad core. Thus, channel I can detect Pb(II) ions while the channel II can detect Cu(II) ions. In the proposed probe, copper and silver are used as the plasmonic materials for realizing SPR for channel I and channel II, respectively. Since two different plasmonic metals have been used for the excitation of surface plasmons, two well-separated SPR absorption bands are expected in the output spectrum, at specific wavelengths (peak absorbance wavelengths) corresponding to the characteristics of each metal. When an aqueous sample of Pb(II) and Cu(II) ions is poured into the flow cell, due to the interaction of metal ions with the sensing layers (metal ion imprinted nanoparticle layers) over the plasmonic films, the effective refractive index of both sensing layers in channel I and channel II changes. This change causes the shift of peak absorbance wavelengths corresponding to both absorption bands due to the phenomenon of SPR. By monitoring the shift in peak absorbance wavelengths, the presence and concentrations of Pb(II) and Cu(II) ions in the aqueous sample can be determined. Figure 3 shows the pictorial representation of the sensing scheme of the sensor.

3.2 *Characterization of Fiber Optic Probe*

A fabricated fiber optic probe was characterized using the experimental setup shown in Fig. 1(b) and discussed in Sec. 2.4. A number of aqueous samples with mixed concentrations of Pb(II) and Cu(II) ions were prepared to record their absorption spectra

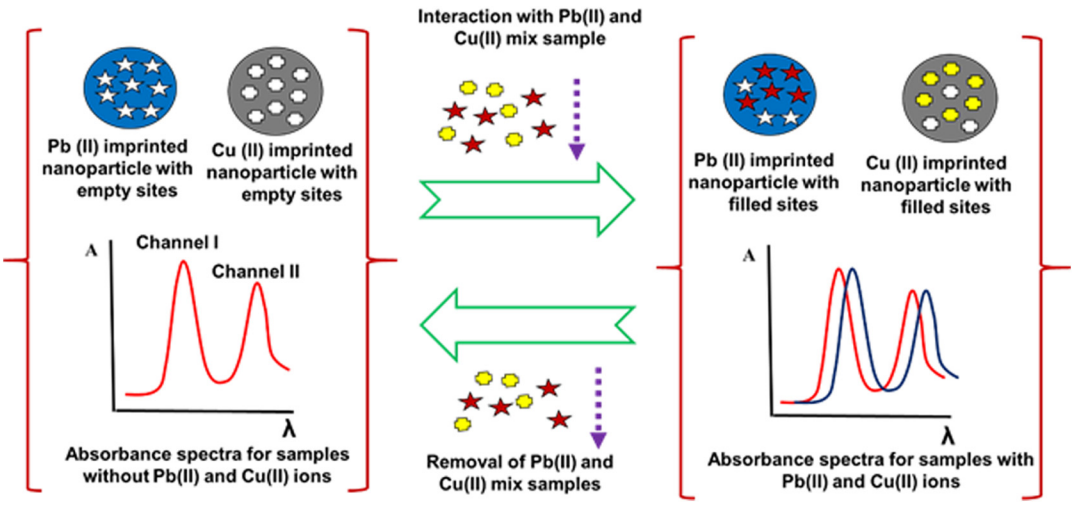

Fig. 3 Pictorial representation of the sensing mechanism for the detection of Pb(II) and Cu(II) ions.

and hence the calibration curves of both channels. The concentrations of Pb(II) and Cu(II) ions in mixed samples were chosen as [0 μg/LPb(II) + 0 mg/LCu(II)], [0.001 μg/LPb(II) + 0.001 mg/LCu(II)], [0.01 μg/LPb(II) + 0.01 mg/LCu(II)], [0.1 μg/LPb(II) + 0.1 mg/LCu(II)], [1 μg/LPb(II) + 1 mg/LCu(II)], [10 μg/LPb(II) + 10 mg/LCu(II)], [100 μg/LPb(II) + 100 mg/LCu(II)], and [1000 μg/LPb(II) + 1000 mg/LCu(II)] covering their presence in various water resources and the human body. Each sample was inserted into the flow cell, and the corresponding absorbance spectrum was recorded using a spectrometer after stabilization. The stabilization takes around 30 s. After that, the sample was extracted from the flow cell and the probe was washed using deionized water, which ensures the removal of any interaction of previous a sample with the sensing region. It should be noted that the cleaning/washing of the probe is essential because if the probe is not cleaned, then the leftover attached analyte ions of a previous sample over the binding sites of the sensor surface would interfere with the results of the next sample since the next sample would get small number of binding sites available for binding. Its effect will add up in the peak

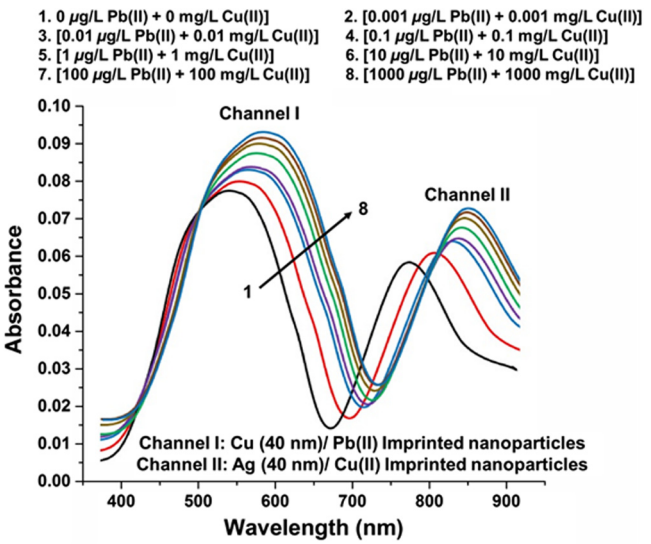

Fig. 4 SPR absorbance spectra of mixed solution for varying concentrations Pb(II) and Cu(II) ions.

absorbance wavelength of the next sample, which will not correspond to the actual concentration of the sample. The absorbance spectra recorded for samples having different concentrations of Pb(II) and Cu(II) ions are shown in Fig. 4. In each spectrum, two absorption bands can be clearly seen: the first corresponds to channel I (Cu metal) while the second is due to channel II (Ag metal). Further, it can be noted that the absorbance bands shift toward higher wavelengths as the concentrations of ions in the mixed sample [Pb(II) and Cu(II)] increase. This is due to the binding of Pb(II) and Cu(II) ions with the corresponding ion-imprinted nanoparticle layers. In channel I, when Pb(II) ions connect with the Pb(II) ion-imprinted nanoparticle layer, they bind with the binding sites present in the nanoparticle layer due to complementary shape and size. The binding causes an increase in the effective refractive index of the nanoparticle layer resulting in the red shift of the SPR absorption band. Similarly, the red shift in the absorption band of channel II is due to the interaction of Cu(II) ions with the Cu(II) ion-imprinted sites synthesized within the nanoparticles.

3.3 *Calibration Curve and Sensitivity*

To calibrate the proposed fabricated probe, the peak absorbance wavelengths were extracted from both absorption peaks of the absorption spectra as shown in Fig. 4. The peak absorbance wavelengths extracted corresponding to different concentrations of both ions have been plotted as the calibration curves of the probe. Figure 5(a) shows the calibration curve of channel I for the detection of Pb(II) ions, whereas Fig. 5(b) represents the calibration curve for channel II for the detection of Cu(II) ions. The shift in peak absorbance wavelength for channel I is obtained to be 30 nm for Pb(II) ion concentration change from 0.001 to 1000 μg/L. For the concentration change from 0 to 1000 μg/L, the observed shift in peak absorbance wavelength is 40 nm. In the case of channel II, the shift in peak absorbance wavelength is 41 nm for the change in Cu(II) ion concentration from 0.001 to 1000 mg/L and is 74 nm for the concentration change from 0 to 1000 mg/L. Both curves saturate at higher concentrations of ions, which is because of the limited number of binding sites on the nanoparticles. For the lower concentration of ions, the binding sites are almost empty, and hence all the ions present in the sensing solution bind with the recognition sites. Thus, the higher shift in peak

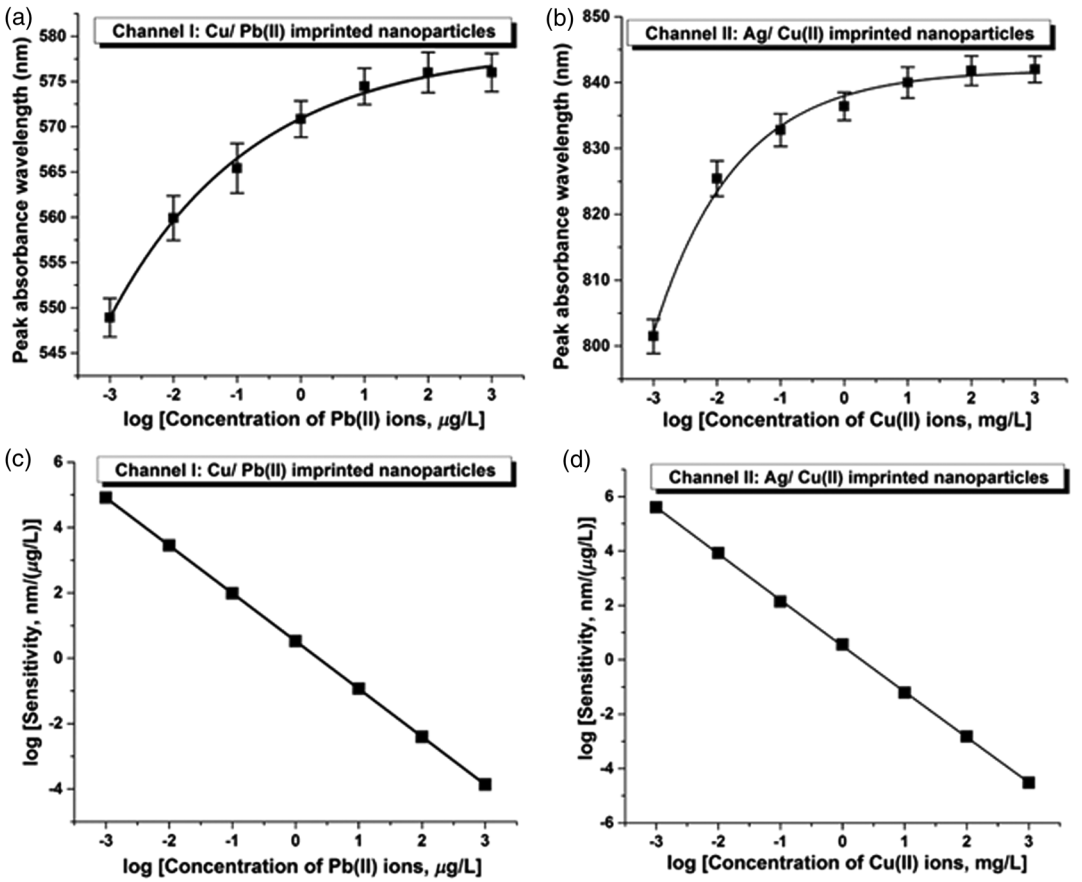

Fig. 5 Calibration curve of (a) channel I and (b) channel II and sensitivity plots of (c) channel I and (d) channel II for the different concentrations of Pb(II) and Cu(II) ions in mixed solutions

absorbance wavelength is observed. Further, as the concentration of ion increases, the number of available imprinted sites per unit ion starts decreasing, which in turn decreases the rate of peak absorbance wavelength shift. At higher concentrations, the binding sites are almost full; thus, no further shift in peak absorbance wavelength occurs on further increase in the concentration of ion, which causes the saturation of the calibration curve at higher concentrations of metal ion. The error bars in Figs. 5(a) and 5(b) show the standard deviation in the peak absorbance wavelength while performing the experiments multiple times. Figures 5(c) and 5(d) show the sensitivities of channel I and channel II with varying concentrations of Pb (II) and Cu(II) ions in mixed solutions, respectively. These have been calculated by taking the derivative of the calibration curves in Figs. 5(a) and 5(b), respectively. The maximum sensitivities have been found to be 8.19×10^4 nm/(μg/L) and 4.07×10^5 nm/(mg/L) for 0.001 μg/L Pb(II) ion concentration and 0.001 mg/L Cu(II) ion concentration, respectively. Such high sensitivities suggest the sensor's main applicability for low concentration of metal ions. It may be noted that the sensitivity of the fabricated probe is highly dependent on the concentration of analyte as can be seen from Figs. 5(c) and 5(d). Its value varies from the order 10^5 to 10^{-4} for the lowest to highest concentrations (10^{-3} to 10^3 concentration unit) of metal ions. Due to large concentration range, the sensitivity and the resonance wavelength have been plotted on the logarithmic scale for both channels, and hence the linear range of operation of the sensor will be negligible. The experiments were carried out a number of times on a single probe and with fresh prepared probes. The variation in the observed peak absorbance wavelength was found to be within the error bars as shown in Figs. 5(a) and 5(b) (calibration curves). This shows the repeatable nature of the fabricated probe.

In the present study, we used Cu and Ag as plasmonic metals. However, in place of Cu, one can also choose Au (gold). It is a widely used material for realizing SPR. There are many studies where Cu has been used because of low cost and its easy immobilization over an unclad core. The coating of Au requires a prior coating of a thin film of chromium (Cr) over an unclad core. Further, the coating of polymeric nanoparticles over Cu is easy compared with Au; due to these reasons, Cu has been preferred over Au in the present study.

Figure 6(a) shows the variation of peak absorbance wavelengths for both channels when aqueous samples of different concentrations of Pb(II) ion only were used for the probe characterization. The figure shows peak absorbance wavelength shift only for the channel I; no variation in peak absorbance wavelength is found for channel II, which results as a horizontal straight line in the plot. Similarly, in the case of aqueous samples of Cu(II) ion only, the peak absorbance wavelength shift is found only for channel II, while a horizontal straight-line variation is observed for channel I as shown in Fig. 6(b). This confirms that the channel I detects only Pb(II) ions and channel II senses Cu(II) ions only. This is because of the highly selective nature of the ion imprinting technology. The binding sites created in polymeric nanoparticle have the complimentary shape

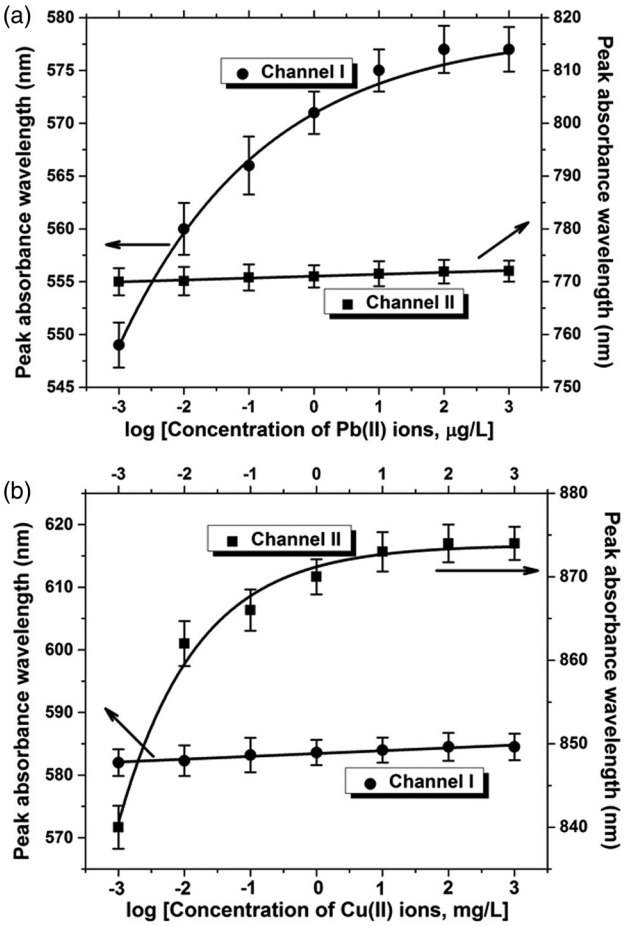

Fig. 6 Peak absorbance wavelength corresponding to channel I and channel II for samples of different concentrations of (a) Pb(II) ions and (b) Cu(II) ions in aqueous solution.

and size of the template ions to be detected. Hence, when that specific template ion comes near these imprinted sites, it interacts and causes the change in effective refractive index of the polymeric nanoparticle layer (sensing layer), which is confirmed by the shift in peak absorbance wavelength observed in the calibration curve. On the other hand, if an ion with a different shape and size comes near the recognition sites, due to different structure, it does not bind with these sites; thus, no shift in peak absorbance wavelength is observed. Hence, the channel I is used only for the sensing of Pb(II) ions while channel II detects Cu(II) ions only.

3.4 *Selectivity*

Selectivity is one of the important performance parameters of any chemical/biosensor. It shows whether the sensor is sensitive toward one specific analyte or a group of analytes. For the selectivity experiments on the proposed probe, samples of various metal ions were prepared and the performance of the fabricated probe was checked using these samples. The metal ions chosen for the selectivity experiments were cobalt [Co(II)], cadmium [Cd(II)], zinc [Zn(II)], and chromium [Cr(II)] apart from lead [Pb(II)] and copper [Cu(II)]. The concentration of each sample was kept as 1 $\mu g/L$. For each sample, the absorbance spectrum was recorded. From the absorbance spectrum of each sample, the peak absorbance wavelength was extracted for both

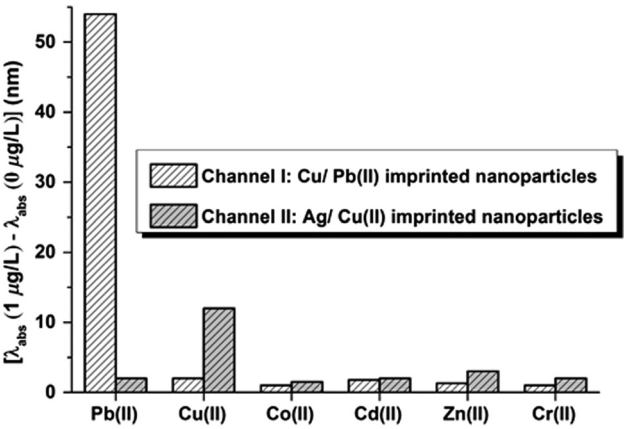

Fig. 7 Selectivity response of channel I and channel II experimenting with samples of different metal ions. The concentration of metal ion solutions is kept as 1 μM.

channels. Similarly, peak absorbance wavelength corresponding to the reference solution (0 $\mu g/L$) was extracted from its absorbance spectrum. Figure 7 shows the bar diagram of the change in peak absorbance wavelength for the change in concentration from 0 to 1 $\mu g/L$ of each sample corresponding to both channels. From the figure, channel I possesses the maximum change in peak absorbance wavelength for Pb(II) ions, whereas channel II shows the maximum change in peak absorbance wavelength for Cu(II) ion. This confirms that the sensing channel I and channel II in the proposed probe are highly selective for the sensing of Pb(II) and Cu(II) ions, respectively. A small change in peak absorbance wavelengths for other analytes (ions) is found due to the physical adsorption of the ions over the sensing layer. The reason for the highly selective nature is the complementary shape and size of the binding site to the template ion to be sensed, which has been discussed in an earlier section.

3.5 *Response Time*

Response times of both channels are determined by measuring the absorbance at peak absorbance wavelengths of each channel as a function of time immediately after pouring the sample in the flow cell. The concentration of mixed sample was chosen as [1 $\mu g/L$Pb(II) + 1 $\mu g/L$Cu(II)]. Figures 8(a) and 8(b) represent the response time plot of channel I and channel II, respectively, and the values of response time determined from these plots for both channels are found to be about 15 s. Thus, the sensor is fast in giving the response.

3.6 *Detection Limit and Quantification Limit*

The limit of detection of a sensor is the minimum analyte concentration that can be detected by the device. It is calculated from the ratio of the spectral resolution of the spectrometer with the sensitivity of the sensor near blank concentration. In our case, the spectral resolution of the spectrometer is 0.333 nm. The sensitivities corresponding to channel I and channel II are 8.19×10^4 nm/($\mu g/L$) and 4.07×10^5 nm/(mg/L) near-zero concentration of Pb(II) and Cu(II) ions, respectively. Thus, the calculated values of LODs for channel I and channel II are found to be 4.06×10^{-12} g/L and $\{8.18 \times 10^{-10}$ g/L$\}$ for Pb(II) and Cu(II) ions, respectively.

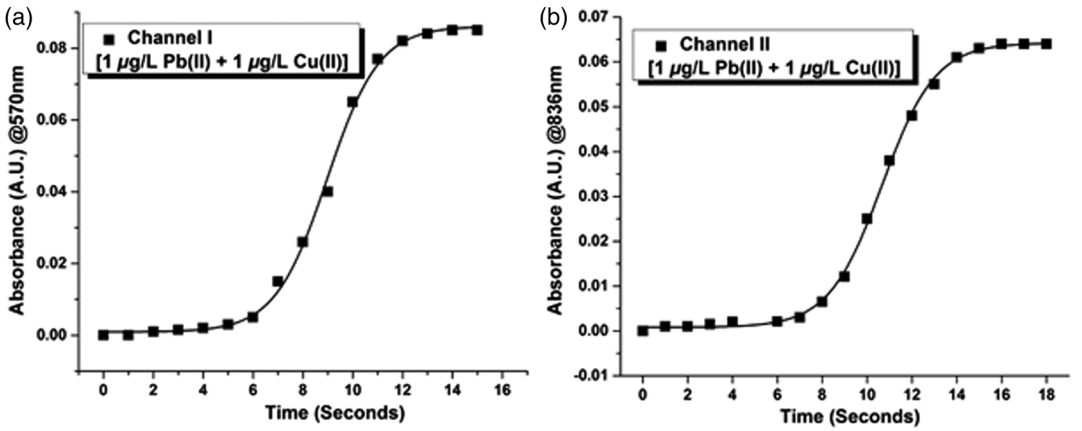

Fig. 8 Response time of (a) channel I and (b) channel II of the fabricated sensing probe.

Table 1 LODs of Pb(II) ion detection methods.

Method	Limit of detection (g/L)	Reference
Colorimetric	2.72×10^{-3}	10
Colorimetric	4.14×10^{-3}	9
Electrochemical	5.46×10^{-6}	15
UV–vis spectroscopy	4.14×10^{-6}	12
Fiber optic SPR+ Pyrrole	4.40×10^{-7}	27
Colorimetric	1.9×10^{-7}	28
RT-PCR technology	1.44×10^{-7}	11
Electrochemical	7×10^{-8}	14
Fiber optic SPR + ion imprinting	4.06×10^{-12}	Present study

Table 2 LODs of Cu(II) ion detection methods.

Method	Limit of detection (g/L)	Reference
Colorimetric	1.26×10^{-3}	9
SPR: chip based	4.14×10^{-3}	29
IR spectroscopy	4.41×10^{-5}	7
Colorimetric	3.2×10^{-6}	30
Electrochemical	6.13×10^{-7}	15
Colorimetric	5×10^{-7}	8
Colorimetric	2.54×10^{-7}	31
Electrochemical	1.89×10^{-8}	32
Electrochemical	2.52×10^{-9}	13
Fiber optic SPR + ion imprinting	8.18×10^{-10}	Present study

Another parameter that is important is the limit of quantification (LOQ). It is the minimum analyte concentration that can be sensed by the device while considering the standard deviation in peak absorbance wavelength. Hence, it is calculated as the ratio of the standard deviation in peak absorbance wavelength and the sensitivity of the sensor near zero concentration. The values of standard deviation in peak absorbance wavelength for both channels were found to be 2.13 and 2.58 nm, respectively. Taking these values, LOQ was calculated and was found to be 2.61×10^{-11} and 6.33×10^{-8} g/L, respectively. A comparison of LOD of our sensing probe with LODs of other reported studies for the detection of Pb(II) and Cu(II) ions was made and is shown in Tables 1 and 2, respectively. From Tables 1 and 2, it can be observed that our proposed sensor possesses the lowest values of LOD for Pb(II) and Cu(II) ions among the other methods to the best of our knowledge.

Although the sensing method has several advantages such as cost effectiveness and simple fabrication steps, it has limitations of the number of channels and ions to be detected. In this study, only two channels have been fabricated over the single optical fiber. This is because of the finite spectral width of the spectrometer. However, the number of sensing channels can be increased if the spectrometer covering broader spectral range and the metals having resonance peaks at higher wavelengths are used. The other limitation is that it can only detect metal ions having a +2 positive charge. In other cases, monomer, cross-linking agent, and method of polymer synthesis would be different.

4 Conclusion

A sensor is designed, fabricated, and characterized for the simultaneous detection of Cu(II) and Pb(II) ions in aqueous samples by cascading two channels in a single fiber optic probe using SPR and ion-imprinted nanoparticles. Channel I is used for the detection of Pb(II) ions while channel II works for the sensing of Cu(II) ions. SPR is realized by coating copper and silver films over two unclad channels (channel I and channel II, respectively). Ion-imprinted nanoparticles of Pb(II) and Cu(II) are used as the sensing layers for the channel I and channel II, respectively. The probe is characterized using the spectral

interrogation method. Due to the presence of two different plasmonic metals, two well-separated absorption bands are found in the output absorbance spectrum. Each band corresponds to the characteristics of one of the sensing channels. The operating ranges of the sensor for Pb(II) and Cu(II) ion samples are 0 to 1000 μg/L and 0 to 1000 mg/L, respectively. Further, the sensitivities of channel I and channel II are 8.19×10^4 nm/(μg/L) and 4.07×10^5 nm/(mg/L) near the lowest concentration of Pb(II) and Cu(II) ion samples, respectively. The detection limits of both channels are found to be lowest in comparison with other studies reported in the literature on sensing of Pb (II) and Cu(II) ions. In addition to simultaneous sensing, the fabricated probe has the advantages of low cost, immunity to the electromagnetic interference, high sensitivity, high selectivity, and capability of online monitoring and remote sensing.

Disclosures

The authors have no conflicts of interest.

Acknowledgments

Anand M. Shrivastav is grateful to UGC (India) for a research fellowship.

References

1. N. Tekaya et al., "Ultra-sensitive conductometric detection of heavy metals based on inhibition of alkaline phosphatase activity from Arthrospiraplatensis," *Bioelectrochemistry* **90**, 24–29 (2013).
2. G. L. Turdean, "Design and development of biosensors for the detection of heavy metal toxicity," *Int. J. Electrochem.* **2011**, 1–15 (2011).
3. L. Patrick, "Lead toxicity. Part II: the role of free radical damage and the use of antioxidants in the pathology and treatment of lead toxicity," *Altern. Med. Rev.* **11**, 114–127 (2006).
4. D. Bagal-Kestwal et al., "Invertase inhibition basedelectrochemical sensor for the detection of heavy metal ions in aqueoussystem: application of ultra-microelectrode to enhance sucrose biosensor's sensitivity," *Biosens. Bioelectron.* **24**, 657–664 (2008).
5. Q. He et al., "A selective fluorescent sensor for detecting lead in living cells," *J. Am. Chem. Soc.* **128**, 9316–9317 (2006).
6. Z. H. Chohan and S. K. A. Sherazi, "Biological role of cobalt(II), copper (II) and nickel(II) metal ions on the antibacterial properties of some nicotinoyl-hydrazine derived compounds," *Met.-Based Drugs* **4**, 69–74 (1997).
7. G. G. Huang and J. Yang, "Selective detection of copper ions in aqueous solution based on an evanescent wave infrared absorption spectroscopic method," *Anal. Chem.* **75**, 2262–2269 (2003).
8. I. Vopálenská, L. Váchová, and Z. Palková, "New biosensor for detection of copper ions in water based on immobilized genetically modified yeast cells," *Biosens. Bioelectron.* **72**, 160–167 (2015).
9. Y. Guo et al., "Colorimetric detection of mercury, lead and copper ions simultaneously using protein-functionalized gold nanoparticles," *Biosens. Bioelectron.* **26**, 4064–4069 (2011).
10. P. Chen et al., "Colorimetric detection of lead ion based on gold nanoparticles and lead-stabilized G-quartet formation," *J. Biomed. Sci. Eng.* **8**, 451–457 (2015).
11. Y. Zhu et al., "Ultrasensitive detection of lead ions based on a DNA-labelled DNAzyme sensor," *Anal. Methods* **7**, 662–666 (2015).
12. N. L. T. Nguyen et al., "Sensitive detection of lead ions using sodium thiosulfate and surfactant-capped gold nanoparticles," *BioChip J.* **10**, 65–73 (2016).
13. P. R. Oliveira et al., "Electrochemical determination of copper ions in spirit drinks using carbon paste electrode modified with biochar," *Food Chem.* **171**, 426–431 (2015).
14. R. Seenivasan, W. J. Chang, and S. Gunasekaran, "Highly sensitive detection and removal of lead ions in water using cysteine-functionalized graphene oxide/polypyrrole nanocomposite film electrode," *Appl. Mater. Interfaces* **7**, 15935–15943 (2015).
15. M. P. N. Bui et al., "Simultaneous detection of ultratrace lead and copper with gold nanoparticles patterned on carbon nanotube thin film," *Analyst* **137**, 1888–1894 (2012).
16. J. Wackerlig and P. A. Lieberzeit, "Molecularly imprinted polymer in nanoparticles in chemical sensing-synthesis, characterization and application," *Sens. Actuators B* **207**, 144–157 (2015).
17. L. Chen, S. Xu, and J. Li, "Recent advances in molecular imprinting technology: current status, challenges and highlighted applications," *Chem. Soc. Rev.* **40**, 2922–2942 (2011).
18. B. D. Gupta, A. M. Shrivastav, and S. P. Usha, "Surface plasmon resonance-based fiber optic sensors utilizing molecular imprinting," *Sensors* **16**, 1381 (2016).
19. A. M. Shrivastav, S. P. Usha, and B. D. Gupta, "Highly sensitive and selective erythromycin nanosensor employing fiber optic SPR/ERY imprinted nanostructure: application in milk and honey," *Biosens. Bioelectron.* **90**, 516–524 (2017).
20. A. Olaru et al., "Surface plasmon resonance (SPR) biosensors in pharmaceutical analysis," *Crit. Rev. Anal. Chem.* **45**, 97–105 (2015).
21. M. Couture, S. S. Zhao, and J. Masson, "Modern surface plasmon resonance for bioanalytics and biophysics," *Phys. Chem. Chem. Phys.* **15**, 11190–11216 (2013).
22. A. K. Sharma, R. Jha, and B. D. Gupta, "Fiber-optic sensors based on surface plasmon resonance: a comprehensive review," *IEEE Sens. J.* **7**, 1118–1129 (2007).
23. R. Tabassum and B. D. Gupta, "Simultaneous estimation of vitamin K_1 and heparin with low limit of detection using cascaded channels fiber optic surface plasmon resonance," *Biosens. Bioelectron.* **86**, 48–55 (2016).
24. R. Verma and B. D. Gupta, "A novel approach for simultaneous sensing of urea and glucose by SPR based optical fiber multianalyte sensor," *Analyst* **139**, 1449–1455 (2014).
25. J. Jia, A. Wu, and S. Luan, "Synthesis and investigation of the imprinting efficiency of ion imprinted nanoparticles for recognizing copper," *Phys. Chem. Chem. Phys.* **16**, 16158–16165 (2014).
26. L. S. Molochnikov et al., "Coordination of Cu(II) and Ni(II) in polymers imprinted so as to optimize amine chelate formation," *Polymer* **44**, 4805–4815 (2003).
27. R. Verma and B. D. Gupta, "Detection of heavy metal ions in contaminated water by surface plasmon resonance based optical fiber sensor using conducting polymer and chitosan," *Food Chem.* **166**, 568–575 (2015).
28. H. Kuang et al., "Rapid and highly sensitive detection of lead ions in drinking water based on a strip immunosensor," *Sensors* **13**, 4214–4224 (2013).
29. R. Wang et al., "Detection of copper ions in drinking water using the competitive adsorption of proteins," *Biosens. Bioelectron.* **57**, 179–185 (2014).
30. Y. R. Ma et al., "Colorimetric detection of copper ions in tap water during the synthesis of silver/dopamine nanoparticles," *Chem. Commun.* **47**, 12643–12645 (2011).
31. N. Pan et al., "Highly sensitive colorimetric detection of copper ions based on regulating the peroxidase-like activity of Au@Pt nanohybrids," *Anal. Methods* **8**, 7531–7536 (2016).
32. T. Wu, T. Xu, and Z. Ma, "Sensitive electrochemical detection of copper ions based on the copper(II) ion assisted etching of Au@Ag nanoparticles," *Analyst* **140**, 8041–8047 (2015).

Anand Mohan Shrivastav received his MSc degree in physics in 2012 from C.S.J.M. University Kanpur (India). Since July 2013, he has been a full-time PhD student at the physics department, Indian Institute of Technology Delhi. He is a UGC (India) research fellow and is a student member of the Optical Society of America (OSA). His research areas of interest are surface plasmon resonance, lossy mode resonance, fiber optic sensors, and molecular imprinting.

Banshi D. Gupta is a professor of physics at the Indian Institute of Technology Delhi. He received his MSc degree in physics from Aligarh Muslim University (India) and his PhD from the Indian Institute of Technology Delhi in 1975 and 1979, respectively. He has published more than 170 research papers in international journals and 100 papers in conferences in the area of plasmonic biosensors, fiber optic sensors, and nanotechnology and has authored three books on sensors.